

HOW FAR ARE THE SOURCES OF ICECUBE NEUTRINOS? CONSTRAINTS FROM THE DIFFUSE TEV GAMMA-RAY BACKGROUND

XIAO-CHUAN CHANG^{1,2}, RUO-YU LIU^{1,3}, XIANG-YU WANG^{1,2}

¹ School of Astronomy and Space Science, Nanjing University, Nanjing, 210093, China; xywang@nju.edu.cn

² Key laboratory of Modern Astronomy and Astrophysics (Nanjing University), Ministry of Education, Nanjing 210093, China

³ Max-Planck-Institut für Kernphysik, 69117 Heidelberg, Germany

Draft version May 19, 2016

ABSTRACT

The nearly isotropic distribution of the TeV-PeV neutrinos recently detected by IceCube suggests that they come from sources at distance beyond our Galaxy, but how far they are is largely unknown due to lack of any associations with known sources. In this paper, we propose that the cumulative TeV gamma-ray emission accompanying the production of neutrinos can be used to constrain the distance of these neutrino sources, since the opacity of TeV gamma rays due to absorption by the extragalactic background light (EBL) depends on the distance that these TeV gamma rays have travelled. As the diffuse extragalactic TeV background measured by *Fermi* is much weaker than the expected cumulative flux associated with IceCube neutrinos, the majority of IceCube neutrinos, if their sources are transparent to TeV gamma rays, must come from distances larger than the horizon of TeV gamma rays. We find that above 80% of the IceCube neutrinos should come from sources at redshift $z > 0.5$. Thus, the chance for finding nearby sources correlated with IceCube neutrinos would be small. We also find that, to explain the flux of neutrinos under the TeV gamma-ray emission constraint, the redshift evolution of neutrino source density must be at least as fast as the the cosmic star-formation rate.

Subject headings: gamma rays–neutrinos

1. INTRODUCTION

The IceCube Collaboration recently announced the discovery of extraterrestrial neutrinos (Aartsen et al. 2013, 2014a, 2015a). The sky distribution of these events is consistent with isotropy (Aartsen et al. 2014a). Such an isotropic distribution could be produced as long as the distance of the source is significantly larger than the size of the Galactic plane, thus extragalactic astrophysical objects are usually proposed as their sources, but a Galactic halo origin is also possible (Taylor et al. 2014). The proposed extragalactic sources include galaxies with intense star-formation (Loeb & Waxman 2006; He et al. 2013; Murase et al. 2013; Liu et al. 2014; Chang & Wang 2014; Tamborra et al. 2014; Chang et al. 2015; Chakraborty & Izaguirre 2015; Senno et al. 2015a; Bartos & Marka 2015), jets and/or cores of active galactic nuclei (AGNs) (Stecker et al. 1991; Kalashev et al. 2014; Kimura et al. 2015; Padovani & Resconi 2014), gamma-ray bursts (Waxman & Bahcall 1997; He et al. 2012; Liu & Wang 2013; Murase & Ioka 2013; Bustamante et al. 2015; Fraija 2015) and etc. The large uncertainty in our current knowledge about the distance of neutrinos is due to that so far no associated astrophysical sources have been identified.

A common way to produce astrophysical high-energy neutrinos is the decay of charged pions created in inelastic hadronuclear (pp) and/or photohadronic ($p\gamma$) processes of cosmic rays (CRs), in which high-energy gamma rays will be also generated from the decay of synchronously created neutral pions. The emissivity of gamma rays and neutrinos are related through $E_\gamma Q_\gamma(E_\gamma) \approx (2/3) E_\nu Q_\nu(E_\nu)|_{E_\nu=E_\gamma/2}$ (for pp process), where Q represents the emission rate per source. VHE gamma rays ($\gg 100$ GeV), unlike neutrinos which propagate through the universe almost freely, will be significantly absorbed by the extragalactic background light (EBL) and cosmic microwave background (CMB) during the propaga-

tion through intergalactic space if the source distance is larger than the mean free path of these gamma rays. For a TeV gamma-ray photon, the optical depth would be larger than unity when the source locates at $z \gtrsim 0.1$. Therefore, the cumulative flux of VHE gamma rays associated with neutrinos carries the information about the distance of the sources of these neutrinos.

Significant progresses have been made in our understanding of the extragalactic gamma-ray background (EGB) in recent years. The spectrum of the EGB has now been measured with the Fermi-LAT in the energy range from 0.1 to 820 GeV (Ackermann et al. 2015a). New studies of the blazar source count distribution at gamma-ray energies above 50 GeV place an upper limit on the residual non-blazar component of the EGB (Ackermann et al. 2015b). In this paper, we use this upper limit at TeV energy to constrain the distance and the evolution of the bulk population of neutrino sources. The distance information has important implications for the search of correlations between observed neutrino events and nearby gamma-ray sources. If the inferred distances of the majority of neutrino sources are large, the search for nearby correlated sources would be a challenge. It may also explain the negative result¹ of search for the correlation between neutrinos and ultra-high energy cosmic rays obtained by (Aartsen et al. 2015b), which originate within $\lesssim 100$ Mpc.

In §2, we first present how we use the TeV emission to place constraints. Then, in §3, we give the input conditions and assumptions. We give our results in §4. Finally, we give the conclusions and discussions in §5.

2. THE METHOD FOR CONSTRAINTS

¹ See however, the result obtained by Moharana & Razzaque (2015), who find that the arrival directions of the cosmic neutrinos are correlated with $\gtrsim 10$ EeV UHECR arrival directions. This can be explained only if the sources are hidden in TeV gamma-rays.

In the astrophysical origin scenarios, neutrinos (also gamma rays) are produced in various discrete astrophysical objects, so the total observed neutrino flux are the sum of contributions of each individual source, rather than from truly diffuse emissions. We assume that the neutrino sources are transparent to TeV gamma rays, and only consider the attenuation in the intergalactic space due to EBL and CMB absorption. For simplicity, we assume here a Poisson distribution for the closest sources², then the probability density that the n -th-closest source locates at a comoving distance r can be expressed as

$$p(n, r) = \frac{4\pi N^{n-1}}{(n-1)!} e^{-N} r^2 \rho_0 \quad (1)$$

where N is the expectation number of the sources within a spherical comoving volume V with radius r , i.e. $N = \int \rho_0 4\pi r^2 dr$. So the expected comoving distance where the n -th-closest source locates is $\bar{r}(n) = \int_0^\infty p(n, r) r dr$. For distant sources, the effect of fluctuation of distances are unimportant and the distribution can be treated as a uniform distribution, i.e. $\rho = \rho(z)$.

The influence of source number density on the gamma ray background is complicated. If the spatial number density of the sources is low, given a measured diffuse neutrino flux, the corresponding pionic gamma ray luminosity of each source should be relatively high, so this kind of sources are easier to be resolved by instruments. By contrast, if the spatial number density of the source is high, the luminosity of each source should be smaller. As a result, these sources are more likely to be unresolved and hence the emitted gamma rays contribute to the isotropic diffuse gamma-ray background (IGRB). If more nearby sources are resolved from background, the distant sources are allowed to be brighter without violating the IGRB data. Such a requirement can be expressed as,

$$\Phi_{\gamma, \text{un}}(E_\gamma) = \sum_{F_n < F_{\text{sens}}}^n F_n(E_\gamma) \leq \Phi_{\text{IGRB}}(E_\gamma), \quad (2)$$

where $\Phi_{\gamma, \text{un}}(E_\gamma)$ represents the cumulative flux of unresolved sources, $F_n(E_\gamma)$ represents the flux of the n -th closest source and F_{sens} is the point source sensitivity of *Fermi*-LAT.

In the same time, the resolved sources contribute to EGB together with the unresolved ones, so they must satisfy

$$\Phi_{\gamma, \text{tot}}(E_\gamma) = \sum^n F_n(E_\gamma) \leq \Phi_{\text{EGB}}(E_\gamma), \quad (3)$$

where $\Phi_{\gamma, \text{tot}}(E_\gamma)$ represents the cumulative flux of all sources, including both resolved and unresolved ones. In our calculation, we use the broadband sensitivity provided by *Fermi*-LAT performance in Pass 8³. Assuming the gamma-ray spectral index $\gamma = 2$, the sensitivity reaches a level of $F_{\text{sens}} \sim 2 \times 10^{-13} \text{ ergs cm}^{-2} \text{ s}^{-1}$. According to this, we can determine whether a point source is resolved or not. Based on the above two requirements (Eqs. 2 and 3), we will study how the maximum neutrino contribution from certain source is constrained by the *Fermi* data.

² The distribution of the closest galaxies may be clumpy, which suggests an overdensity of the nearby sources. Since the total mass fraction in the nearby universe is small, we find that this overdensity hardly affects our results.

³ http://www.slac.stanford.edu/exp/glast/groups/canda/lat_Performance.htm

For simplicity, we assume that all the sources have the same intrinsic gamma-ray luminosity L' , which relates to the gamma-ray spectral emissivity $Q'_\gamma(E'_\gamma)$ by $L' = \int_{E'_{\text{min}}}^{E'_{\text{max}}} Q'_\gamma(E'_\gamma) dE'_\gamma$, where E'_{max} and E'_{min} are the maximum and minimum energy of emitted photons respectively. Here the prime denotes quantities measured in the rest frame of the source (i.e., $E'_\gamma = E_\gamma(1+z)$). While low-energy gamma rays can propagate to us from the sources freely, VHE gamma rays may be absorbed by the EBL and CMB photons in the intergalactic space. The produced electron/positron pairs will also interact with EBL and CMB photons and generate secondary gamma rays by inverse-Compton scattering. Such a cycle is called cascade, and it will continue until the newly generated photons are not energetic enough to produce electron/positron pairs by interacting with the background photons. As a result, the absorbed high-energy gamma rays are reprocessed to a bunch of lower-energy ones. So the total gamma ray flux after propagation consists of a primary component which is the unabsorbed gamma rays, and a cascade component, i.e.,

$$F(E_\gamma) = \left\{ Q'_\gamma[(1+z)E_\gamma] e^{-\tau(E_\gamma)} + Q_{\gamma, \text{cas}}(E_\gamma) \right\} / 4\pi \bar{r}^2, \quad (4)$$

where $\tau(E_\gamma)$ is the optical depth for a photon of energy E_γ . In this paper, we use the optical depth provided by Finke et al. (2010)⁴ and discuss the effect of other EBL models later.

Since the results depend on the density of the neutrino source, we will consider three different cases:

1) High-density source case, such as star-forming/starburst galaxies. The density of starburst galaxies is about $4 \times 10^{-4} \text{ Mpc}^{-3}$. Starburst galaxies, due to their high star formation rates, and hence large number of supernova or hypernova remnants therein, are huge reservoirs of cosmic ray (CR) protons with energy up to EeV (Wang et al. 2007). These CRs produce high-energy neutrinos by colliding with gases in galaxies (Loeb & Waxman 2006; Liu et al. 2014).

2) Middle-density case, such as clusters of galaxies. The density of clusters of galaxies is about $\sim 10^{-6} - 10^{-5} \text{ Mpc}^{-3}$ depending on the mass selection (Jenkins et al. 2001). Here we choose $4 \times 10^{-6} \text{ Mpc}^{-3}$ as a reference value. Galaxy clusters have been argued to be able to accelerate CRs and considered as possible sources for high-energy neutrinos (Murase et al. 2008).

3) Low-density case, such as blazars (e.g. BL Lacs and flat-spectrum radio quasars (FSRQs)). Their density ranges from 10^{-9} Mpc^{-3} to 10^{-7} Mpc^{-3} (Ajello et al. 2012, 2014). We choose $4 \times 10^{-8} \text{ Mpc}^{-3}$ as a reference value. As blazars are powerful gamma-ray sources, there have been extensive discussions about their possibility of being high-energy neutrino sources (see Ahlers & Halzen (2015) for a review).

It should be noted that the three densities we chose are just reference values to study the effect of different source density. Any specific sources should refer to the corresponding results based on their spatial densities.

3. ASSUMPTION ABOUT THE EXTRAGALACTIC NEUTRINO FLUX AND INJECTION SPECTRA OF GAMMA RAYS

The latest combined maximum-likelihood analysis of IceCube neutrinos gives a best-fit power law spectrum with a spectral index of $\gamma = 2.50 \pm 0.09$ in the energy range between 25 TeV and 2.8 PeV, and an all-flavor flux of $\phi =$

⁴ <http://www.phy.ohiou.edu/~finke/EBL/index.html>

$(6.7^{+1.1}_{-1.2}) \cdot 10^{-18} \text{GeV}^{-1} \text{s}^{-1} \text{sr}^{-1} \text{cm}^{-2}$ at 100 TeV (Aartsen et al. 2015a). Interestingly, The IceCube collaboration has tested the hypothesis of isotropy by analyzing data in the northern and southern sky respectively. Compared to the all-sky result, the spectrum of the events in the northern sky can be better fitted by a harder power-law ($\gamma = 2.0^{+0.3}_{-0.4}$), while the southern one favors a slightly softer spectrum ($\gamma = 2.56 \pm 0.12$). However, the result is not conclusive, as the discrepancy could be simply caused by a statistical fluctuation. Alternatively, it could be due to an additional component that is present in only one of the hemispheres (either an unmodeled background component, or e.g. a component from the inner Galaxy).

As indicated in some recent studies (Ackermann et al. 2015b), the EGB above 50 GeV is dominated by blazars at a level of $86^{+16}_{-14}\%$. These are mostly low-luminosity hard-spectrum BL Lacs. If it is correct, this implies a strong suppression of contributions from other sources, which can contribute at most a flux of $\lesssim 2-3 \times 10^{-8} \text{GeV cm}^{-2} \text{s}^{-1} \text{sr}^{-1}$ at 50 GeV. If the neutrino sources are transparent to gamma rays, the neutrino flux per-flavor is then constrained to be at most $\sim 10^{-8} \text{GeV cm}^{-2} \text{s}^{-1} \text{sr}^{-1}$, which can explain the measured neutrino flux at PeV energy, but is insufficient to explain the flux at ~ 25 TeV. To solve this tension, it has been proposed that TeV neutrinos may come from some hidden sources, i.e. they are not transparent to gamma rays (Murase et al. 2016; Bechtol et al. 2015).

Considering the above uncertainties, we divide our discussions into two cases. In the first case, we adopt the non-blazar EGB obtained by Ackermann et al. (2015b) to place constraints. We assume that the gamma-ray background is only relevant to $\gtrsim 100$ TeV neutrinos whose sources are transparent to gamma-rays and ~ 25 TeV neutrinos may originate from some hidden sources or from a component of the inner Galaxy. Possible hidden sources were suggested (Stecker et al. 1991; Murase et al. 2016; Tamborra & Ando 2016; Senno et al. 2016; Wang & Liu 2016). The gamma-ray spectrum at the source should follow the spectrum of neutrinos, which is assumed to be a flat spectrum with index $\gamma = 2.0$ below 1 PeV, as predicted by the Fermi acceleration mechanism, and a steeper spectrum with $\gamma = 2.5$ above 1 PeV (Aartsen et al. 2014a). Then the injection spectrum of gamma rays can be expressed as

$$\begin{cases} Q_\gamma(E_\gamma) \propto E_\gamma^{-2}, E_\gamma < 2(1+z)\text{PeV} \\ Q_\gamma(E_\gamma) \propto E_\gamma^{-2.5}, E_\gamma \geq 2(1+z)\text{PeV}. \end{cases} \quad (5)$$

In the second case, we relax this requirement by considering the full EGB given in Ackermann et al. (2015a), allowing blazars to contribute to IceCube neutrinos. The neutrino spectrum at the source is assumed to follow a broken power law with the spectral index $\gamma = 2$ at $E_\nu < 25$ TeV and $\gamma = 2.5$ at $E_\nu > 25$ TeV (Aartsen et al. 2015a). Then the injection spectrum of gamma rays can be expressed as

$$\begin{cases} Q_\gamma(E_\gamma) \propto E_\gamma^{-2}, E_\gamma < 50(1+z)\text{TeV} \\ Q_\gamma(E_\gamma) \propto E_\gamma^{-2.5}, E_\gamma \geq 50(1+z)\text{TeV}. \end{cases} \quad (6)$$

4. RESULTS

When the cumulative TeV flux is fixed, as constrained by the IGRB and EGB data, the total neutrino flux is affected by two factors. First, as we already mentioned above, the spatial density of the sources is an important factor. If the density is smaller, the luminosity of individual source is larger and hence more nearby sources will be resolved. Gamma rays

from these resolved sources will not be counted into IGRB while they still contribute to diffuse neutrino flux. The second factor is the distance of the source or the evolution of the source density with redshift. TeV photons from more distant sources will be more likely to be absorbed during propagation to the earth, while neutrinos will not. So the neutrino flux will be higher if the fraction of distant sources is higher (or the density evolution with redshift is stronger). In our calculation, we adopt two forms of redshift evolution for the purpose of illustration: one is the constant density evolution, which means that the comoving density of the sources does not change with redshift; the other one is the star formation rate (SFR) evolution, for which the source density evolves as $\propto (1+z)^{3.4}$ at $z < 1$, $\propto (1+z)^{-0.3}$ at $1 < z < 4$ and $\propto (1+z)^{-3.5}$ at $z > 4$ (Hopkins & Beacom 2006; Yüksel et al. 2008).

4.1. Non-blazar EGB case

In this case, we assume that EGB and IGRB are only relevant to $\gtrsim 100$ TeV neutrinos and adopt the non-blazar EGB obtained by Ackermann et al. (2015b) as an upper limit of the cumulative gamma-ray flux from neutrino sources. First, we want to study what fraction of the observed neutrino flux is contributed by nearby sources. In Fig. 1, we fix the limit of gamma-ray flux to be $2.5 \times 10^{-9} \text{GeV cm}^{-2} \text{s}^{-1} \text{sr}^{-1}$ at 820 GeV, which corresponds to 14% of the total EGB (i.e., the non-blazar EGB⁵), and calculate the maximally allowed neutrino flux at PeV as a function of the boundary distance z_{max} . The boundary distance z_{max} means that all the sources contributing to IGRB/EGB locate within the redshift z_{max} . The spectra of gamma rays and neutrinos are assumed to follow Eq. (5).

The left panel of Fig. 1 shows the maximally allowed neutrino flux at 1 PeV without violating the non-blazar EGB. The figure indicates that, in all three source density cases, only a small fraction of neutrinos come from low redshift sources. The sources below $z_{\text{max}} = 0.5$ can account for at most a fraction of 20% of the total neutrino flux. Thus, the majority of neutrinos observed by IceCube should come from distance farther than $z = 0.5$. We can also see that, to account for the observed neutrino flux, the redshift evolution of the sources should not be slower than that of the cosmic star formation rate (SFR). The constant evolution with respect to redshift can be ruled out. The above discussions only consider the constraints by the TeV gamma-ray background. However, in the low source density case, the nearest point sources could have been detected by IceCube, given a sensitivity of $E^2 dE/dN \sim 10^{-12} \text{TeV s}^{-1} \text{cm}^{-2}$ for IceCube (Aartsen et al. 2014b). So we should also consider the constraints by IceCube observation. This extra constraint suggests that the source density should not be too low, unless part of gamma ray emissions of the sources does not come from the same hadronic process that produces neutrinos. Considering the latter possibility for the low-density source case and the constraint by IceCube non-detection of nearby sources, we re-calculate the maximum neutrino flux, which is shown in the right panel of Fig. 1. We find that the extra constraint affects the low density case and the requirement of a fast evolution is strengthened.

The requirement of a fast evolution of the source density with redshift can also be seen by comparing the expected cumulative TeV gamma-ray emission accompanying the pro-

⁵ Ackermann et al. (2015b) find that blazars constitute about 86% of the integrated photon flux above 50 GeV. We here assume the spectrum of the summed emission of all blazars are identical to that of the observed EGB.

duction of neutrinos with the observed gamma-ray background data. Fig. 2 shows the cumulative gamma-ray emission for different redshift evolution scenarios. Here we adopt the high source density case for illustration, while the result holds for other source density cases. We can see that a faster redshift evolution will lead to a steeper gamma-ray spectrum. Since Ackermann et al. (2015b) provide only the fraction of integral contribution to the total EGB above 50 GeV by blazars, the exact fraction of non-blazar EGB flux at 820 GeV is unclear. Thus, we draw a series of horizontal lines in Fig. 2 to show the different levels of the non-blazar EGB fraction at 820 GeV. If the non-blazar EGB flux is lower than $\lesssim 14\%$ of the total EGB flux at 820 GeV, the source evolution is required to be faster than that of SFR. In all three density evolution scenarios, however, the flux at 10-100 GeV are quite similar, which is naturally expected since 10-100 GeV gamma rays are almost as transparent as neutrinos. This demonstrates the unique role of TeV gamma-ray flux in constraining the evolution of neutrino source density.

4.2. Full EGB case

In this case, we allow blazars to contribute to IceCube neutrinos and use the full EGB as the upper limit (Ackermann et al. 2015a). The IGRB constraint becomes important for this case and we need to consider this constraint as well. Thus, we fix the upper limits of the cumulative gamma-ray flux at 820 GeV to be $6 \times 10^{-9} \text{GeVcm}^{-2}\text{s}^{-1}\text{sr}^{-1}$ for unresolved sources (IGRB) and $3 \times 10^{-8} \text{GeVcm}^{-2}\text{s}^{-1}\text{sr}^{-1}$ for all the sources (EGB).

First, we assume that 10–100 TeV neutrinos originate from extragalactic sources that are transparent to TeV gamma rays. Fig. 3 shows the maximally allowed neutrino flux at ~ 25 TeV as a function of the boundary redshift z_{max} , by assuming a gamma-ray spectrum of Eq. (6). The result suggests a similar preference for high-redshift sources. In the high and middle density cases, the source density evolution should not be slower than the cosmic SFR evolution. Since the luminosities of these sources are relatively low, we find that IceCube non-detection constraint hardly affect the result. On the other hand, for the low density case, the observed neutrino flux can be achieved even for a constant source density evolution. However, when considering the neutrino non-detection constraint of nearby point sources, only $\lesssim 15\%$ of the EGB flux at 820 GeV can be associated with neutrinos from the same hadronic process. Including this extra constraint by IceCube non-detection, we find that the source evolution should be faster than the SFR evolution for the low-density case, as shown in the right panel of Fig. 3. Like in the non-blazar case, we compare the cumulative gamma-ray emission of unresolved sources with the IGRB data in Fig. 4 for the high source density case. We find that, in order not to exceed the IGRB at 820 GeV, the source density must evolve faster than the SFR evolution.

However, it has been suggested that the EGB above 50 GeV is dominated by low-luminosity hard-spectrum BL Lacs (Ackermann et al. 2016), which have a negative evolution with redshift in source density (Ajello et al. 2014). If this is correct, we can exclude the possibility that these BL Lacs are the main sources of 10-100 TeV neutrinos observed by IceCube. This is consistent with the conclusion in a previous study by summing up neutrino flux from individual BL Lacs (Padovani et al. 2015). Thus, the tension between the fact that the dominant sources producing the gamma-ray back-

ground have negative evolution with redshift and our conclusion that the sources of the high energy neutrinos must have a fast, positive evolution with redshift argues for hidden sources for 10-100 TeV neutrinos. Meanwhile, we should also note that some types of blazars such as FSRQs, have a fast, positive evolution with redshift and they only contribute a small part of EGB/IGRB flux. These sources are still possible sources for $\gtrsim 100$ TeV IceCube neutrinos. This is consistent with the recent discovery of a PeV neutrino which is in temporal and positional coincidence with a high-fluence outburst from the FSRQ PKS B1424-418 at redshift $z = 1.522$ (Kadler et al. 2016). For these FSRQs, the situation is actually quite similar to the low-density sources in the non-blazar case.

5. DISCUSSIONS AND CONCLUSIONS

In the above calculation, we used the EBL model given by Finke et al. (2010). Different EBL models might affect the opacity of TeV gamma rays and we thus study this effect. We use the upper and lower bounds on the opacity given by Stecker (2013) as the boundary of EBL uncertainties. Fig. 5 shows the influence on cumulative gamma-ray emission when varying the EBL opacity within this boundary. For illustration, we adopt a local source density of $4 \times 10^{-4} \text{Mpc}^{-3}$ with the SFR evolution. We find that, even for the strongest EBL intensity model, the cumulative TeV flux decreases only slightly (less than 20%) compared to the case using the EBL model given by Finke et al. (2010). Thus, we conclude that the uncertainty from EBL models does not change our conclusion that a fast source density evolution is required.

In previous sections, we obtained the constraint on the source density evolution assuming that the gamma-ray (or neutrino) luminosity is the same for all sources. If the gamma-ray/neutrino luminosity of the source also varies with redshift, it is then the gamma-ray/neutrino emission rate density, rather than source number density, that is constrained. The emission rate density can be expressed as $g(z)\rho(z)$, where $\rho(z)$ represents the source number density and $g(z)$ is the factor accounting for the luminosity evolution of the source. As long as their product $g(z)\rho(z)$, has a fast evolution with redshift, the requirement is fulfilled. So the source number density may not need to evolve that fast if the factor $g(z)$ evolves fast enough. The factor $g(z)$ could originate from various physical causes. For example, in the starburst galaxy scenario for IceCube neutrinos, cosmic rays may have a higher pion production efficiency in higher-redshift galaxies due to higher gas densities therein, which leads to a larger $g(z)$ at higher redshifts (Chang et al. 2015). Besides, we note that, although high-luminosity hard-spectrum BL Lacs show only a mild evolution in the redshift range of $1 < z < 2$, they are severely deficient in low-redshift ($z < 0.5$) universe (Ajello et al. 2014). These sources can be essentially regarded as a fast evolution case, so they may avoid the excess in the diffusive TeV gamma-ray background when accounting for IceCube neutrinos.

To summarize, we find that extragalactic TeV gamma-ray background is a useful tool to study the distance and density evolution of neutrino sources. We have considered blazar and non-blazar source models and used different injection spectra correspondingly. In both cases, we find that only a small fraction of neutrinos are allowed to come from low-redshift sources in order not to exceed the diffuse TeV gamma-ray background limit. To account for the IceCube neutrino flux, the density of neutrino sources must have a fast evolution with redshift. Interestingly, this is consistent with the independent result obtained by the tomographic constraints (Ando et al.

2015). In addition, even for a fast source density evolution, only $\gtrsim 100$ TeV neutrino flux could be explained. As our result shows that the IceCube neutrinos mainly come from distant sources at high redshifts, any models arguing for nearby sources may be ruled out as long as these sources are transparent to TeV gamma rays. Also, any search for nearby sources correlated with IceCube neutrinos would face a challenge. Instead, we suggest to search for correlations with potential cosmic ray accelerators at high redshifts.

We thank Paolo Padovani for the discussions and the anonymous referee for the invaluable report. This work is supported by the 973 program under grant 2014CB845800, the NSFC under grants 11273016, and the Excellent Youth Foundation of Jiangsu Province (BK2012011).

REFERENCES

- Aartsen, M. G., Abbasi, R., Abdou, Y., et al. 2013, *Physical Review Letters*, 111, 021103
- Aartsen, M. G., Ackermann, M., Adams, J., et al. 2014a, *Physical Review Letters*, 113, 101101
- Aartsen, M. G.; Ackermann, M.; Adams, J.; et al., 2014b, *ApJ*, 796, 109
- Aartsen, M. G., Abraham, K., Ackermann, M., et al. 2015a, *ApJ*, 809, 98
- Aartsen, M. G., Abraham, K., et al. 2015b, arXiv:1511.09408
- Ackermann, M., Ajello, M., Albert, A., et al. 2015, *ApJ*, 799, 86
- Ackermann et al. 2015b, arXiv:1511.00693
- Ackermann, M., Ajello, M., Atwood, W. B., et al. 2016, *ApJS*, 222, 5
- Ahlers, M., & Halzen, F. 2014, *Phys. Rev. D*, 90, 043005
- Ahlers, M., & Halzen, F. 2015, *Reports on Progress in Physics*, 78, 126901
- Ajello, M., Shaw, M. S., Romani, R. W., et al. 2012, *ApJ*, 751, 108
- Ajello, M., Romani, R. W., Gasparrini, D., et al. 2014, *ApJ*, 780, 73
- Ando, S., Tamborra, I., & Zandanel, F. 2015, *Physical Review Letters*, 115, 221101
- Bartos, I., & Marka, S. 2015, arXiv:1509.00983
- Bechtol, K., Ahlers, M., Di Mauro, M., Ajello, M., & Vandenbroucke, J. 2015, arXiv:1511.00688
- Bustamante, M.; Baerwald, P.; Murase, K.; Winter, W., 2015, *Nature Communications*, 6, 6783
- Chakraborty, S., & Izaguirre, I. 2015, *Physics Letters B*, 745, 35
- Chang, X.-C., & Wang, X.-Y. 2014, *ApJ*, 793, 131
- Chang, X.-C., Liu, R.-Y., & Wang, X.-Y. 2015, *ApJ*, 805, 95
- Finke, J. D., Razzaque, S., & Dermer, C. D. 2010, *ApJ*, 712, 238
- Frajia, N. 2015, arXiv:1508.03009
- He, H. N.; Liu, R. Y., Wang, X. Y., Nagtaki, S., Murase, K. & Dai, Z. G., 2012, *ApJ*, 752, 29
- He, H.-N.; Wang, T.; Fan, Y.-Z.; Liu, S.-M.; Wei, D.-M., *Phys. Rev. D*, 87, 063011
- Hopkins, A. M., & Beacom, J. F. 2006, *ApJ*, 651, 142
- Jenkins, A., Frenk, C. S., White, S. D. M., et al. 2001, *MNRAS*, 321, 372
- Kadler, M., Krauß, F., Mannheim, K., et al. 2016, *Nature Physics*, in press, arXiv:1602.02012
- Kalashhev, O., Semikoz, D., & Tkachev, I. 2014, arXiv:1410.8124
- Kimura, S. S., Murase, K., & Toma, K. 2015, *ApJ*, 806, 159
- Liu, R.-Y., Wang, X.-Y., 2013, *ApJ*, 766, 73
- Liu, R.-Y., Wang, X.-Y., Inoue, S., Crocker, R., & Aharonian, F. 2014, *Phys. Rev. D*, 89, 083004
- Loeb, A., & Waxman, E. 2006, *JCAP*, 5, 3
- Moharana, R., & Razzaque, S. 2015, *JCAP*, 8, 014
- Murase, K., Inoue, S., & Nagasaki, S. 2008, *ApJ*, 689, L105
- Murase, K., Ahlers, M., & Lacki, B. C. 2013, *Phys. Rev. D*, 88, 121301
- Murase, K., & Ioka, K. 2013, *Physical Review Letters*, 111, 121102
- Murase, K., Guetta, D., & Ahlers, M. 2016, *Phys.Rev.Lett.* 116, 071101
- Padovani, P., & Resconi, E. 2014, *MNRAS*, 443, 474
- Padovani, P., Petropoulou, M., Giommi, P., & Resconi, E. 2015, *MNRAS*, 452, 1877
- Senno, N., Mészáros, P., Murase, K., Baerwald, P., & Rees, M. J. 2015, *ApJ*, 806, 24
- Senno, N., Murase, K., & Meszaros, P. 2016, *Phys. Rev. D* 93, 083003
- Stecker, F. W., Done, C., Salamon, M. H., & Sommers, P. 1991, *Physical Review Letters*, 66, 2697
- Stecker, F. W. 2013, arXiv:1302.2065
- Tamborra, I., Ando, S., & Murase, K. 2014, *JCAP*, 9, 043
- Tamborra, I., & Ando, S. 2016, *Phys. Rev. D* 93, 053010
- Taylor, A. M., Gabici, S., & Aharonian, F. 2014, *Phys. Rev. D*, 89, 103003
- Wang, X.-Y., Razzaque, S., Mészáros, P., & Dai, Z.-G. 2007, *Phys. Rev. D*, 76, 083009
- Wang, X.-Y., & Liu, R.-Y. 2016, *Phys. Rev. D*, 93, 083005
- Waxman, E., & Bahcall, J. 1997, *Physical Review Letters*, 78, 2292
- Yüksel, H., Kistler, M. D., Beacom, J. F., & Hopkins, A. M. 2008, *ApJ*, 683, L5

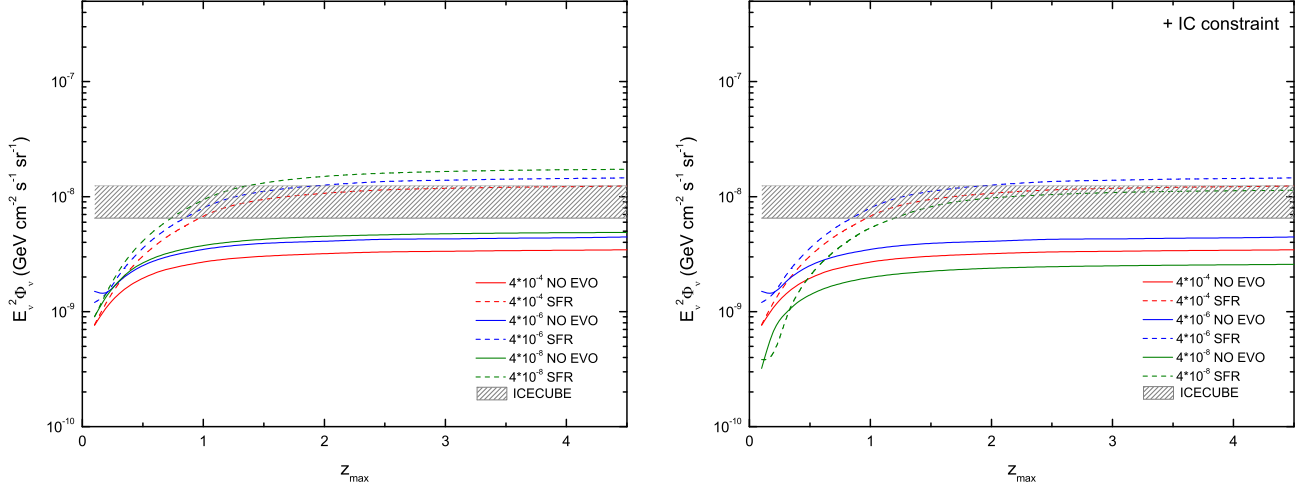


Figure 1. The maximally-allowed neutrino flux at 1 PeV under the constraint of the non-blazar TeV gamma-ray background as a function of the boundary redshift z_{\max} in the non-blazar source case. The red, blue and green lines represent the cases with source density of $4 \times 10^{-4} \text{Mpc}^{-3}$, $4 \times 10^{-6} \text{Mpc}^{-3}$ and $4 \times 10^{-8} \text{Mpc}^{-3}$, respectively. The solid and dashed lines represent, respectively, no evolution and SFR evolution of the source density with redshift. The grey shaded area represents the observed neutrino flux (per flavor) by IceCube at 1 PeV with errors (Aartsen et al. 2014a). In the right panel, an extra constraint due to the IceCube non-detection of nearest point sources is considered.

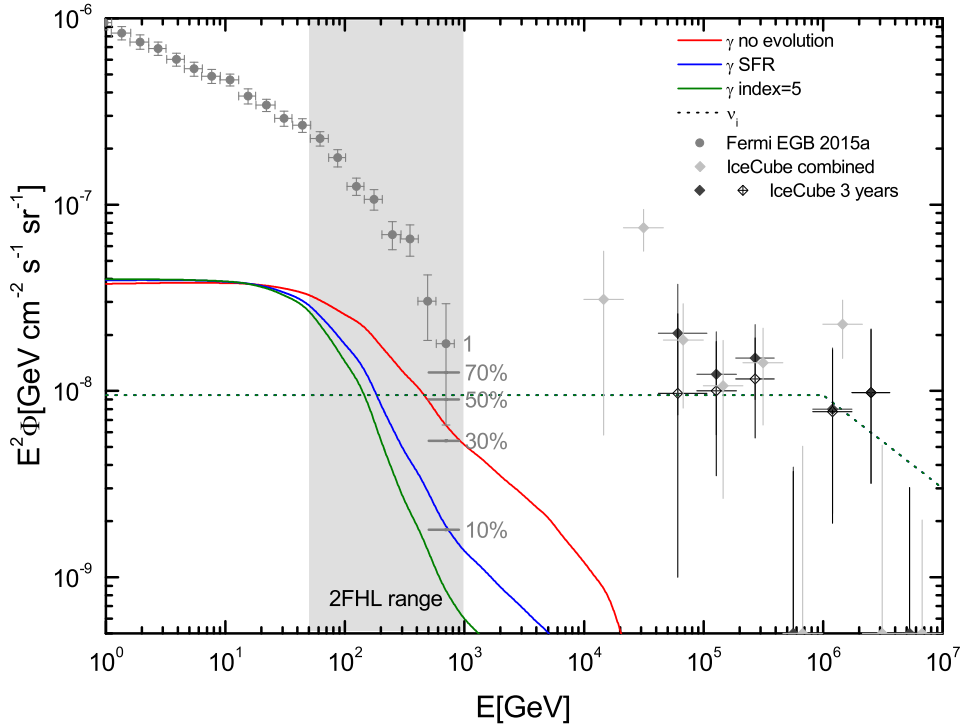


Figure 2. The cumulative gamma-ray emission associated with production of IceCube neutrinos in non-blazar case for different redshift evolution models. The spectrum of the neutrinos used in the calculation is shown by the short dashed line. The red, blue and green lines show, respectively, the cases assuming no redshift evolution, SFR evolution and an evolution given by $\propto (1+z)^5$ at $z < 1$, $\propto (1+z)^{-0.3}$ at $1 < z < 4$, and $\propto (1+z)^{-3.5}$ at $z > 4$. The IGRB data from *Fermi*-LAT are denoted by grey dots and the horizontal short grey lines shows 10%, 30%, 50% and 70% of EGB flux at 820 GeV, respectively (Ackermann et al. 2015a). The IceCube data are denoted by black and grey dots (Aartsen et al. 2014a, 2015a). In the calculation, we use the case of source density of $4 \times 10^{-4} \text{Mpc}^{-3}$.

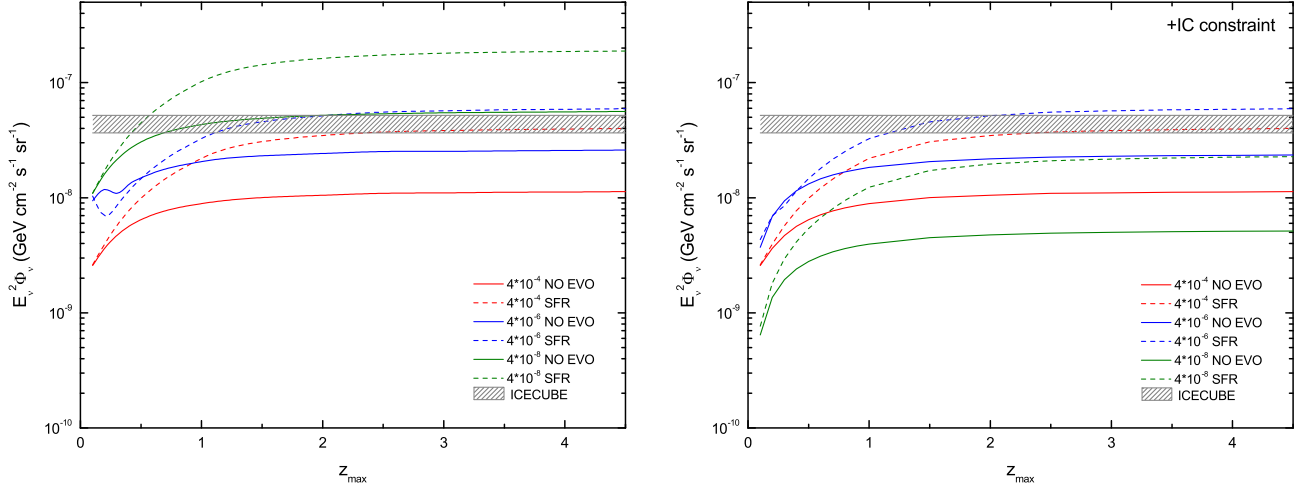


Figure 3. Same as Figure 1, but for the full EGB case. Note that all the neutrino fluxes here correspond to the values at the reference energy of 25 TeV. The horizontal shaded region corresponds to the observed neutrino flux at 25 TeV in the combined analysis (Aartsen et al. 2015a).

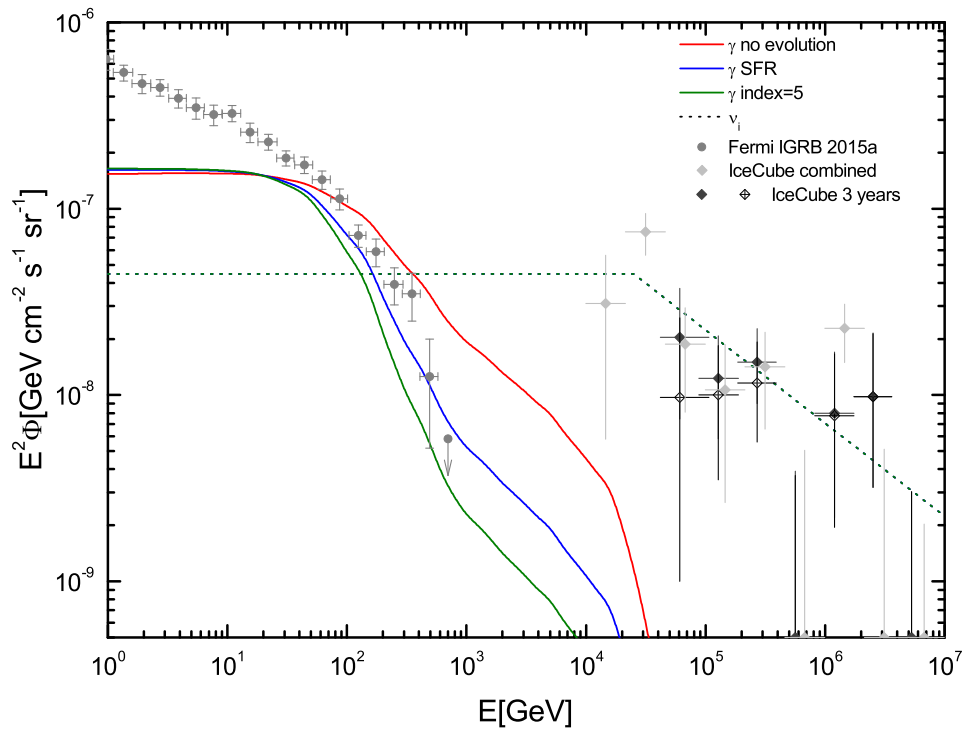


Figure 4. Comparison between the cumulative gamma-ray emission of unresolved sources and the IGRB data for different density evolution models. In the calculation, we use the case of source density of $4 \times 10^{-4} \text{Mpc}^{-3}$. The neutrino flux data are denoted by black and grey dots.

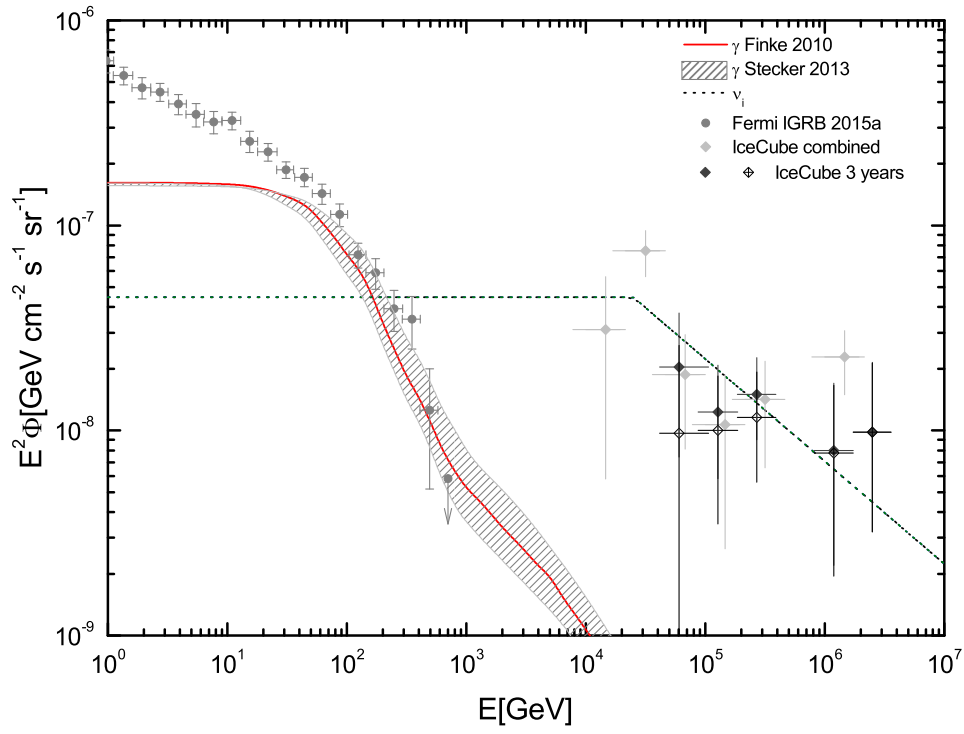


Figure 5. Same as figure 4, but considering the uncertainty in EBL models. We use the upper and lower bounds on the opacity given by Stecker (2013) as the boundary of EBL uncertainties. The red line shows the gamma-ray emission corresponding to the EBL model provided by Finke et al. (2010). In the calculation, we use a source density of $4 \times 10^{-4} \text{Mpc}^{-3}$ and assume SFR redshift evolution.